

Dehazing of Images using Minimum White Balance Optimization



Deoyani Mujbaile, Dinesh Rojatkhar

Abstract: The quality of image captured in presence of fog and haze is degraded due to atmospheric scattering. In order to restore such images, several dehazing algorithms have been proposed. These algorithms sometimes, results in either a contrast distorted dehazed image or a dehazed image that has influence of dense haze. In order to solve this problem, dynamic facsimile dehaze system built on minimum white balance optimization is proposed. This paper proposed a system that integrates some famous single image dehazing algorithms and enhance their outputs using histograms and adaptive histograms; then adaptively select the output with minimum white balance distortion in order to get the optimum output. Experimental results demonstrated that the presented system can attain better dehazing effect and further improves universality of dehazing methods. Also proposed system improves luminance and contrast of dehazed images to a certain extent.

Keywords: Adaptive histogram equalization, contrast distorted, dynamic, histogram equalization.

I. INTRODUCTION

Weather conditions degrades the quality of capture image by absorption, scattering and reflection; restricting and influencing effective use of different types of onsite visual arrangements. Different types of weather conditions have different effects on image depending on type, size and concentration of particles [1]; and can be listed as haze [2], fog [3], cloud [4], rain [4] and snow [4]. Amongst all these, considering clouds will be of no use for ground based visual systems and rain as well as snow changes spatial and temporal characteristics of image; requiring completely different analysis mechanism. Thus, our work concentrates on haze and fog. Also, with mutations of the climate and ever-increasing air pollution, frequency of occurrence of hazy weather has increased. Hence, investigation on haze and dehaze of facsimile are of prominent empirical significance. Dehazing algorithms can also be applied in real time processing applications and these real time processing applications have great market value.

Revised Manuscript Received on June 30, 2020.

* Correspondence Author

Deoyani Mujbaile*, Department of Electronics Engineering, Government College of Engineering Amravati, Amravati, Maharashtra. Email: mujbaileda23@gmail.com

Dinesh Rojatkhar, Department of Electronics Engineering, Government College of Engineering Amravati, Amravati, Maharashtra. Email: dinesh.rojatkhar@gmail.com

© The Authors. Published by Blue Eyes Intelligence Engineering and Sciences Publication (BEIESP). This is an open access article under the CC BY-NC-ND license (<http://creativecommons.org/licenses/by-nc-nd/4.0/>)

The aerosols and water droplets present in fog and haze degenerates image owing to scattering [5]. Scattering leads to mechanism of attenuation and airlight, which are major causes of hazy image. Attenuation causes seeming brightness of captured facsimile to decrease with path length. Direct transmission is the term used for attenuated flux that reaches camera [1]. The attenuated irradiance at a point p located at distance d from observer [6] is given as

$$E(d, \lambda) = \frac{I_o(\lambda) r e^{-\beta(\lambda)d}}{d^2}$$

Where, λ is wavelength of incident light

$I_o(\lambda)$ is radiant intensity at point of origin

r is cone of sky visible from point of origin

$\beta(\lambda)$ is total scattering coefficient

Airlight causes seeming brightness of captured facsimile to increase with path length. The irradiance of airlight at point p located at distance d from observer [7] is given as

$$L(d, \lambda) = L_h(\infty, \lambda)(1 - e^{-\beta(\lambda)d}) \quad (2)$$

Where, $L_h(\infty, \lambda) = k$ is maximum radiance at horizon. "Equation (2)" implies that at $d = 0$; i.e.; for objects closer to observer, airlight is zero or object appears clear.

Countless preliminary image dehazing procedures were built on non-model image dehazing methods; including contrast enhancement algorithms [8]-[11] and Retinex image enhancement algorithms [12]-[13]. However, as crucial process of enforcement of haze to image mutation was not considered, these procedures could not accomplish real sense of dehazing. Thus, researchers have started exploring the image dehazing procedures built on atmospheric scattering model [1] and [14]-[16]. This model is the classic description for the generation of hazy image as

$$I(x) = J(x)t(x) + A(1 - t(x)) \quad (3)$$

Where $I(x)$ is observed hazy image, $J(x)$ is the dehazed irradiance to be recovered, A is global atmospheric light and $t(x)$ is the direct transmission (also called as transmissivity). "Equation (3)" can be re written for dehazed image as

$$J(x) = \frac{1}{t(x)} I(x) - A \frac{1}{t(x)} + A \quad (4)$$

Almost all the existing model based dehaze procedures can be categorized into two major classes: those built on multiple images and those built on single image. The multiple image-based method [6] and [17] uses multiple images to accomplish the task and often require some additional depth information. On the other hand,

single image-based methods [18]-[20] accomplishes the task using only one image and have achieved some significant advantages because of use of strong priors and assumptions. To make potential use of characteristics of mentioned algorithms, this paper proposed a dynamic single facsimile dehaze method built on minimum white balance. This method can dehaze and select best dehazed image using white balance value of dehazed images as metric.

II. DEHAZING METHODS

In this paper we are considering single image-based methods incorporating: Tarel et al.'s algorithm [18], He et al.'s algorithm [19] and Meng et al.'s algorithm [20].

A. Tarel et al.'s restoration algorithm

Tarel et al. has utilized the theory of median filtering and Koschmieder's law to provide a fast dehazing algorithm. The scene radiance of haze free image is given as

$$R(x, y) = \frac{I(x, y) - V(x, y)}{1 - \frac{V(x, y)}{W}} \quad (5)$$

Where, (x, y) is pixel location of interest

$I(x, y)$ is intensity of captured hazy image

$R(x, y)$ is intensity of dehazed image

$V(x, y)$ is atmospheric veil

W is white balance of image caused due to airlight

White colour in captured image is because of presence of haze or fog and in most of the cases, it is estimated by biasing the image average colour towards pure white. Two median filtering operatives have been used for estimation of atmospheric veil as

$$V(x, y) = \max(\min(pB(x, y), W(x, y)), 0) \quad (6)$$

Where, $W(x, y) = \min_{c \in \{r, g, b\}} I^c(x)$ is the minimum value of captured image for that particular colour channel c corresponding to red (r), green (g), blue (b) component and

$$B(x) = C(x) - \text{median}(|W - C(y)|) \quad (7)$$

$$\text{Where, } C(x) = \text{median}(W(y)) \text{ for } p \leq 1 \text{ and } y \in \Omega(x) \quad (8)$$

p denotes a degree of restoration and is an invariable set between [0.9, 0.95] and Ω is the window size for median filtering centred at x . This atmospheric veil, is sometimes, also called a coarse atmospheric scattering value. Thus, a restored image can be obtained by putting estimated values of $V(x)$ and W of "(5)". Use of median filtering appends the exact amount of noise in dehazed facsimile. To overcome this and to obtain final results, smoothing and tone mapping is being performed.

B. He et al.'s restoration algorithm

He et al.'s has used atmospheric scattering model along with strong prior knowledge for developing a dehazing algorithm using single image. This algorithm estimates thickness of haze, recovers good quality of haze free image and provides high quality transmission map. The value of dark channel image is calculated as

$$J^{dark} = \min_{c \in \{r, g, b\}} (\min_{y \in \Omega(x)} (J^c(y))) \quad (9)$$

Where, Ω denotes window centered at x

For haze free image, for sky area and white patches, $J^{dark} \approx 0$

He et al., based on their observations, applied minimum operator on both sides of "(3)" to obtain

$$\min_{c \in \{r, g, b\}} (\min_{y \in \Omega(x)} (\frac{I^c(y)}{A_{\infty}^c})) = t(x) \min_{c \in \{r, g, b\}} (\min_{y \in \Omega(x)} (\frac{I^c(y)}{A_{\infty}^c})) + (1 - t(x)) \quad (10)$$

Combining "(9)" and "(10)", the direct transmission is obtained as

$$\hat{t}(x) = 1 - \min_{c \in \{r, g, b\}} (\min_{y \in \Omega(x)} (\frac{I^c(y)}{A_{\infty}^c})) \quad (11)$$

Using minimum filtering results in blocking effect in the dark channel image, which in turn results in a halo effect on the restored facsimile. To overcome this, soft matting operation is used to optimize transmissivity. Thus, image is restored as

$$J(x) = \frac{I(x) - A_{\infty}}{\max(t(x), t_0)} + A_{\infty} \quad (12)$$

Where, $t(x)$ denotes optimized transmissivity and t_0 denotes a small constant in order to avoid $J(x) \rightarrow \infty$ if $t(x) \rightarrow 0$. Also, A_{∞} is the atmospheric light selected by selecting top 0.1% of the brightest pixel in a local area on the dark channel image.

This approach has certain limitations. The proposed method fails in case of large sky area and dense haze. Also optimized transmissivity obtained using soft matting made time for and is not applicable practically. To avoid this, He et al. proposed guide filtering method as an option to soft matting. The experimental results showed that new algorithm is more efficient than soft matting.

C. Meng et al.'s restoration algorithm

Meng et al. has optimized transmissivity by adopting a regularization-weighted norm and imposing an intrinsic boundary constraint on transmissivity. This work is based on a simple observation.

From (3) it can be supposed that, a pixel $I(x)$ will be contaminated by fog or haze if value of $I(x)$ is impelled to A . So, haze-free pixel $J(x)$ can be obtained by linear extrapolation from A to $I(x)$. The appropriate amount of extrapolation is given by

$$\frac{1}{t(x)} = \frac{\|J(x) - A\|}{\|I(x) - A\|} \quad (13)$$

This algorithm further exhibits that, for given value of x , the extrapolation of $J(x)$ must be sited in radiance cube confined by C_0 and C_1 , where, C_0 and C_1 are two constant vectors. This regulations on $J(x)$ imposes a boundary constraint on $t(x)$, for each x as

$$0 \leq t_b(x) \leq t(x) \leq 1 \quad (14)$$

The transmission $\hat{t}(x)$ is invariable in local patch of facsimile and can be determined by using minimum filtering as

$$\hat{t}(x) = \min(\max t_b(z)) \quad (15)$$

where, $z \in W_x$ and W_x is a local patch centered at x .

Using assumption that, pixels in same blotch shares equal depth value, (11) has been obtained. But in some cases, this assumption fails creating halo effects in restored image.

To circumvent this, a weighting function $W(x)$ is instigated on constraint as

$$W(x)(t(x) - t(y)) \approx 0 \quad (16)$$

Where, x and y are neighboring pixels.

The optimized transmittivity, estimated in this way, is then utilized to estimate unknown radiance of scene.

III. PROPOSED SYSTEM

When the imaging equipment captures image in environment occupied by haze or fog, usually, degradation of image takes place and such an image is called as hazy image. Hazy images occur because of scattering caused by particles present in atmosphere. The performance of various customer and algorithmic photography applications and machine vision system applications is based on captured image. So, biased low contrast radiance of hazy images affects performance of such algorithms. Thus, dehazing can benefit many vision algorithms and advanced image editing. The dehazing algorithms mentioned above had non-identical effects in considering non-identical degraded images. Based on the traits of hazy facsimile, each algorithm mentioned above has its own advantages and disadvantages. Proposed work tries to utilize advantages of each of these algorithms to design a more flexible and generic adaptive dehazing method.

There are different types of image caliber assessment routines [21] available, and each routine has its own traits. According to the traits of the facsimile precision determination, this paper categorized the distorted images as hazy images [21] and used different dehaze algorithms to design an optimum dehazing algorithm. Due to occupancy of fog or haze reproduced facsimile will have whiter component in it and is called as white balance (W_B). W_B is present because haze or fog is white in color. So, less the white balance better is the dehazing and vice versa. Our work uses W_B of dehazed image of different methods as a factor to decide as to which dehazed image should be produced at output.

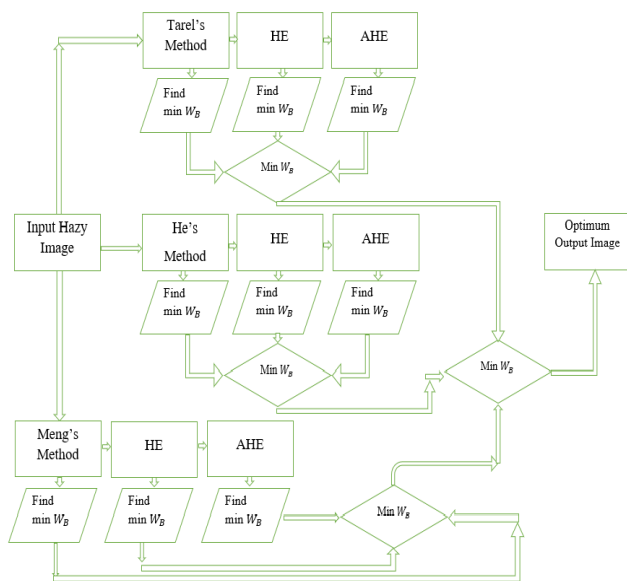


Fig. 1. Schematic Drawing of Proposed System

“Fig.1” showed is the main process of adaptive dehazing. First the identified hazy image is taken as input. All the dehazing algorithms mentioned above will be implemented on this input image and white balance is estimated for dehazed output of each algorithm. After that histogram equalization (HE) and adaptive histogram equalization (AHE) is being performed on output of each dehazing algorithm, in order to further enhance its output. Thus, for each algorithm we will have three outputs; one of original algorithm, second after performing histogram equalization and third after performing adaptive histogram equalization. Thus, in total we have nine images at the end of process. White balance is estimated for all these nine images. Thus, we will have nine white balance values. All these values are compared to obtain minimum (min) value and the image with this minimum white balance is being produced as output.

Histogram equalization and adaptive equalization is a routine to equalize the dispersal of probability of appearance of grey levels in the facsimile [22]. Due to equalization the dynamic range of traits increases without shifting the intrinsic content of the facsimile. In proposed work, these methods are used in order to enhance or sharpen features of images after dehazing.

IV. EXPERIMENTAL RESULTS

Proposed work can be implemented on hazy images of any size. As the size of image increase, the time taken for implementation also increases. In order to maintain consistency, we have considered all input images of equal size.

A. Qualitative Results

For verifying the accuracy and effectiveness of proposed system, hazy images habitually used in studies is being utilized. Intel core processor and PC machine with dominant frequency of 4GHz are being utilized as platforms. The Windows 10 is utilized as operating environment and Matlab2014a is adopted for experimentation of proposed work.

“Fig. 2” shows comparison of results on aerial view of Buildings. From “Fig. 2(a)” and “Fig. 2(k)” it can be concluded that proposed algorithm is selecting optimum result. Thus, algorithm can be applied in case of surveillance using drones in intelligence agencies and government agencies. Also, proposed algorithm can be applied in commercial photography capturing aerial views.

“Fig. 3(k)” and “Fig. 6(k)” are evident that our algorithm works with good efficiency even in case of images having similar color scheme. Thus, it can be used to note afforestation or deforestation by forest departments.

From “Fig. 4(k)” we can say that proposed work can be used in archeological departments for maintenance of historical monuments by using or comparing images of the same captured even under bad weather conditions.

“Fig. 5” shows that our work can also be used to identify objects of same color distinctly and with efficiency even if original image is being distorted by fog.

“Fig 7” shows that algorithm can be applied in case of indoor images and images having quite bright color schemes.

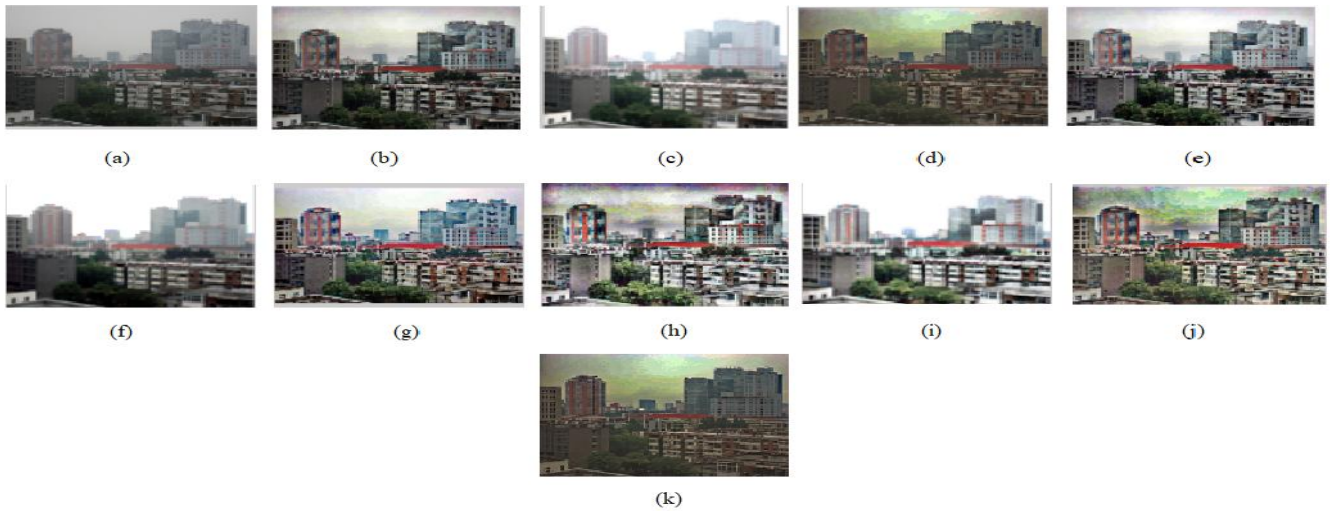


Fig. 2. Comparison of results on the Building image. (a) Input image. (b) Tarel Dehazed image [18]. (c) He Dehazed image [19]. (d) Meng Dehazed image [20]. (e) Tarel HE Dehazed image. (f) He HE Dehazed image. (g) Meng HE Dehazed image. (h) Tarel AHE Dehazed image. (i) He AHE Dehazed image. (j) Meng AHE Dehazed image. (k) Optimum Output image.

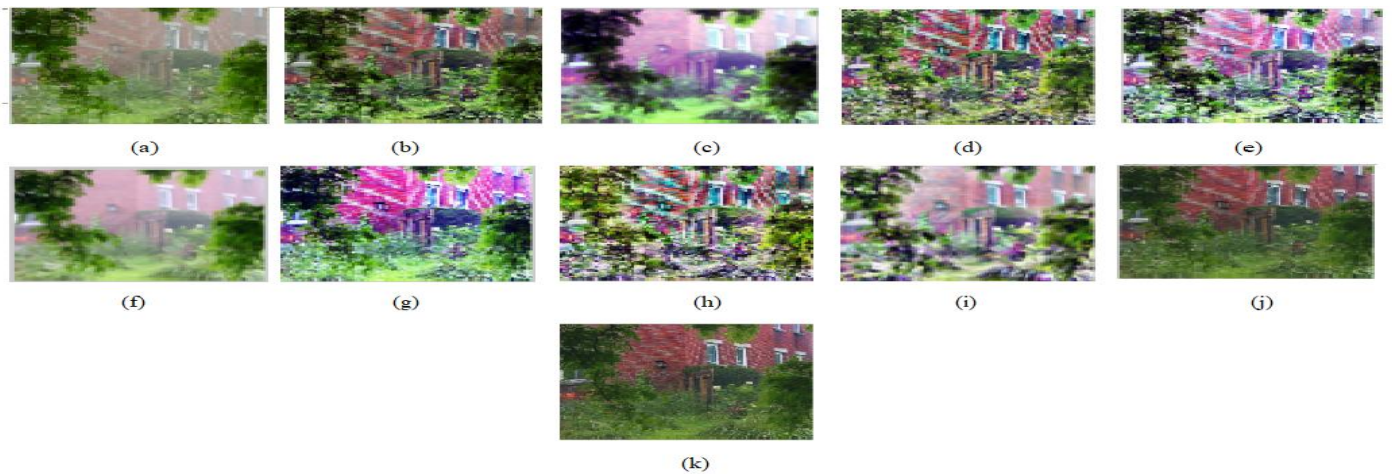


Fig. 3. Comparison of results on the Tree image. (a) Input image. (b) Tarel Dehazed image [18]. (c) He Dehazed image [19]. (d) Meng Dehazed image [20]. (e) Tarel HE Dehazed image. (f) He HE Dehazed image. (g) Meng HE Dehazed image. (h) Tarel AHE Dehazed image. (i) He AHE Dehazed image. (j) Meng AHE Dehazed image. (k) Optimum Output image.

B. Quantitative Results

In order to evaluate the effectiveness of proposed system, this section provides white balance (W_B) values of mentioned algorithms and showed how adaptively our algorithm is adapting lowest value of the same. The results are being tabulated in Table I below. Table I shows white balance values of input images, dehazed images, dehazed images after Histogram Equalization (HE) and of dehazed images after

Adaptive Histogram Equalization (AHE). It can be verified from Table I that white balance values of hazy input images are more than that of dehazed images because of presence of haze or fog in previous one. In other words, white balance of images is used as metric to evaluate amount of restoration and to show effectiveness of our algorithm in adaptively selecting the output.

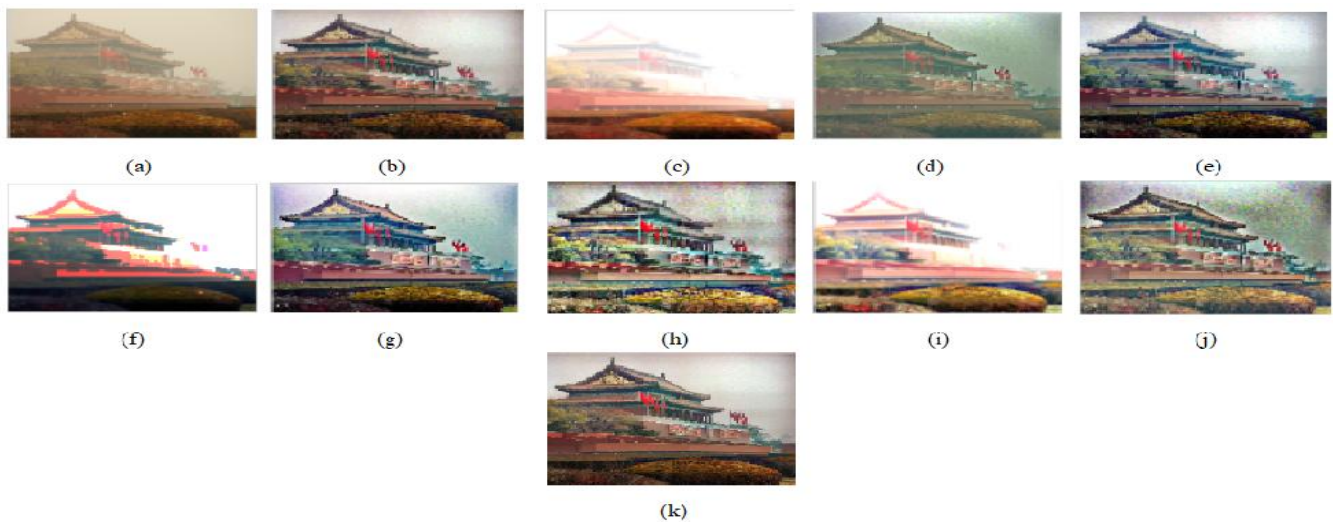


Fig. 4. Comparison of results on the Temple image. (a) Input image. (b) Tarel Dehazed image [18]. (c) He Dehazed image [19]. (d) Meng Dehazed image [20]. (e) Tarel HE Dehazed image. (f) He HE Dehazed image. (g) Meng HE Dehazed image. (h) Tarel AHE Dehazed image. (i) He AHE Dehazed image. (j) Meng AHE Dehazed image. (k) Optimum Output image.

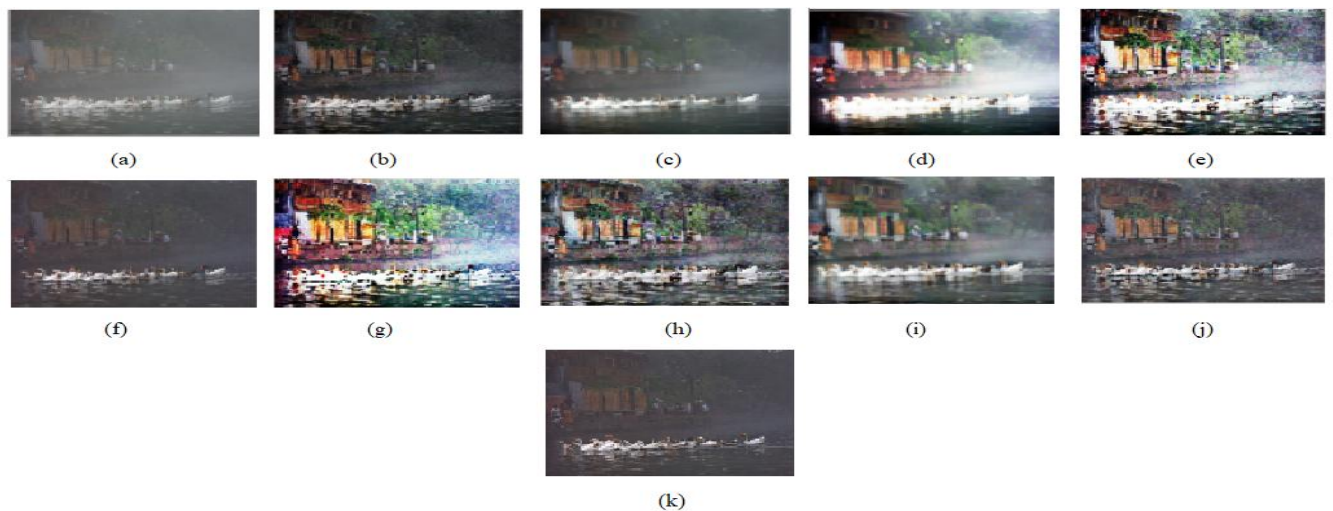


Fig. 5. Comparison of results on the Lake image. (a) Input image. (b) Tarel Dehazed image [18]. (c) He Dehazed image [19]. (d) Meng Dehazed image [20]. (e) Tarel HE Dehazed image. (f) He HE Dehazed image. (g) Meng HE Dehazed image. (h) Tarel AHE Dehazed image. (i) He AHE Dehazed image. (j) Meng AHE Dehazed image. (k) Optimum Output image.

Table- I: White Balance Values for Different Images

Image Name	W_B of Input Image	W_B of Dehazed Images Using									W_B of Output Image
		Tarel	He	Meng	Tarel HE	He HE	Meng HE	Tarel AHE	He AHE	Meng AHE	
Building	1833	748	1184	594	847	776	683	1184	942	1128	594
Tree	1882	1181	1181	1119	872	990	1052	889	1028	672	672
Temple	1566	860	3301	3301	1178	1264	1159	1142	931	1832	860
Lake	3323	273	2236	2236	1229	188	1086	1539	2050	833	188
Hay	1391	950	1335	1335	690	733	654	316	856	852	316
Toys	861	869	1546	1546	731	1006	863	903	991	1025	731

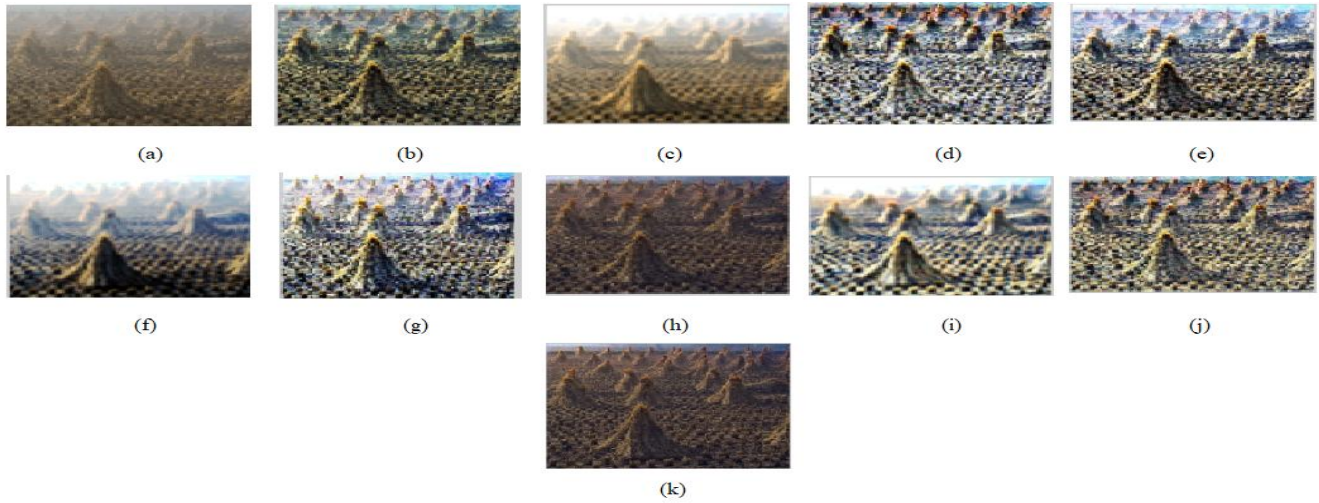


Fig. 6. Comparison of results on the Hay image. (a) Input image. (b) Tarel Dehazed image [18]. (c) He Dehazed image [19]. (d) Meng Dehazed image [20]. (e) Tarel HE Dehazed image. (f) He HE Dehazed image. (g) Meng HE Dehazed image. (h) Tarel AHE Dehazed image. (i) He AHE Dehazed image. (j) Meng AHE Dehazed image. (k) Optimum Output image.

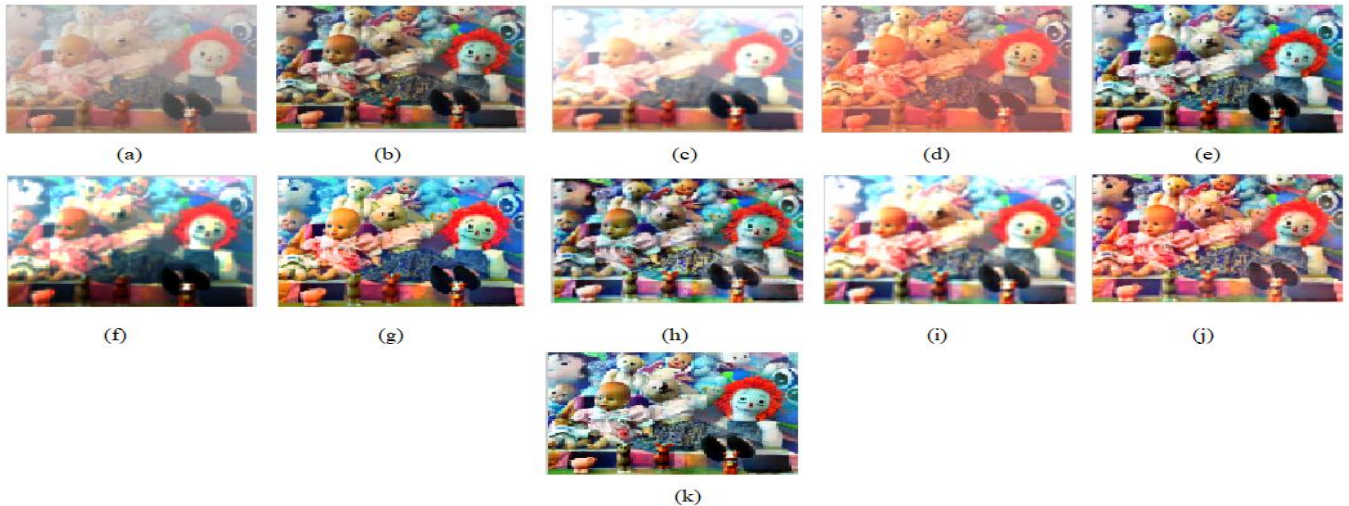


Fig. 7. Comparison of results on the Hay image. (a) Input image. (b) Tarel Dehazed image [18]. (c) He Dehazed image [19]. (d) Meng Dehazed image [20]. (e) Tarel HE Dehazed image. (f) He HE Dehazed image. (g) Meng HE Dehazed image. (h) Tarel AHE Dehazed image. (i) He AHE Dehazed image. (j) Meng AHE Dehazed image. (k) Optimum Output image.

From above Table I it is clear that, algorithm is selecting image with minimum white balance value as output image. It can be noted that input images given has a varying range of white balance values. Thus, algorithm works efficiently for input images having haze or fog of different amounts.

C. Processing Time

Table II shown below tabulates processing delay and selection delay. Processing delay is the time taken by mentioned methods to dehaze hazy images; whereas, selection delay is the time taken by proposed algorithm to select optimum output. Total delay will be the sum of selection delay and processing delay. From table 2 it can be concluded that processing delay is much greater than

selection delay. Thus, designed adaptive selection algorithm is time efficient as well.

Table- II: Processing Delay, Selection Delay, Total Delay

Image Name	Processing Delay (sec)	Selection Delay (sec)	Total Delay (sec)
Building	34.6248	0.3508	34.9756
Tree	20.8334	0.2118	21.0452
Temple	37.5591	0.2512	37.8103
Lake	42.0941	0.2838	42.3779
Hay	18.2577	0.2265	18.4842
Toys	17.6324	0.3158	17.9482

V. CONCLUSION

A dynamic single image dehazing algorithm is extended in this paper using minimum white balance optimization. The algorithm first analyzed input hazy image using existing popular dehazing algorithms to obtain dehazed images. Further histogram equalization and adaptive histogram equalization is performed to further enhance dehazing results. Finally, optimum dehazed image is produced at output using white balance as metric. After simulation, it could be verified that proposed algorithm has better ability and higher stability. Also, ocular caliber of the dehazed image is ameliorated. This paper also gives the probable area of application of proposed system along with example of each in result section.

REFERENCES

1. E. J. McCartney, "Optics of the Atmosphere: Scattering by Molecules and Particles," John Wiley and Sons, New York, 1967.
2. G. M. Hidy, "Aerosols and Atmospheric Chemistry," Academic Press, New York, 1972.
3. J. N. Myers, "Fog," Scientific American, pages 75-82, December 1968.
4. B. J. Manson, "Clouds, Rain and Rainmaking," Cambridge University Press, Cambridge, 1975.
5. M. Minnaret, "The Nature of Light and Color in the Open Air," Dover, New York, 1954.
6. S. K. Nayar and S. G. Narasimhan, "Chromatic Framework for Vision in Bad Weather," in Proc. IEEE Transaction International Conference Computer Vision Pattern Recognition, 2000, pp. 598-605.
7. S. K. Nayar and S. G. Narasimhan, "Vision in Bad Weather," in Proc. IEEE Transaction International Conference Computer Vision, 1999, pp. 802-827.
8. Guo F, Cai Z X and Xie B, "Review and Prospect of Image Dehazing Techniques," Journal of Computer Applications, vol. 30, No. 9, 2010, pp. 2417-2421.
9. Zhu P, Zhu H and Qian X M, "An Image Clearness Method for Fog," Journal of Image and Graphics, vol. 9, No. 1, 20004, pp. 124-128.
10. Zhai Y S, Liu X M and Ya-Yuan T U, "An Improved Fog-Degraded Image Clearness Algorithm," Journal of Dalian Maritime University, vol. 33, No. 3, 2007, pp. 55-58.
11. Wang P, Zhang C and Luo Y X, "Fast Algorithm to Enhance Contrast of Fog-Degraded Images," Journal of Computer Applications, vol. 26, No. 1, 2006, pp. 152-161.
12. Land E H, "The Retinex Theory of Color Vision," Scientific American, vol. 237, No. 6, 1977, pp. 108.
13. S. Parihar and K. Singh, "A Study on Retinex Based Methods for Image Enhancement," Second International Conference on Inventive Systems and Control, 2018, pp. 619-624.
14. S. K. Nayar and S. G. Narasimhan, "Contrast Restoration of Weather Degraded Images," IEEE Transaction on Pattern Analysis and Machine Intelligence (PAMI), 2003, pp. 713-724.
15. R. Tan, "Visibility in Bad Weather from a Single Image," IEEE Conference on Computer Vision and Pattern Recognition, 2008.
16. S. K. Nayar and S. G. Narasimhan, "Vision and the Atmosphere," International Journal of Computer Vision, vol. 48, No. 3, 2002. Pp. 233-254.
17. Y. Y. Schechner, S. K. Nayar and S. G. Narasimhan, "Instant Dehazing of Images Using Polarization," IEEE International Conference on Computer Vision Pattern Recognition, 2001, pp. 325-332.
18. J. P. Tarel and N. Hautiere, "Fast Visibility Restoration from a Single Color Gray Level Image," International Conference on Computer Vision, 2009, pp. 2201-2208.
19. K. He, J. Sun and X. Tang, "Single Image Haze Removal Using Dark Channel Prior," IEEE Conference on Computer Vision and Pattern Recognition, 2009.
20. G. Meng, Y. Wang and J. Duan, "Efficient Image Dehazing with Boundary Constraint and Contextual Regularization," International Conference on Computer Vision, 2013, pp. 616-624.
21. Y. Lang, K. Zhao, W. Zhang and Y. Li, "A Self-Adaption Single Image Dehaze Method Based on Clarity-evaluation-function of Image," International Conference on Advanced Mechatronic Systems, 2018.
22. S. Patel and M. Goswami, "Comparative Analysis of Histogram Equalization Techniques," IEEE International Conference on Contemporary Computing and Informatics, 2014.
23. D. Mujbaile and D. Rojatk, "Model Based Dehazing Algorithms for Hazy Image Restoration – A Review," 2nd International Conference on Innovative Mechanisms for Industry Applications, 2020.

AUTHORS PROFILE



Deoyani Mujbaile received her B.E. and M.Tech Degrees from the University of Nagpur and Amravati, in 2017 and 2020, respectively. Her research interests include Image processing and dehazing. The author has published her research paper in IEEE conference related to Dehazing of Images.



Dinesh Rojatk received his M.E. degree in Electronics Engineering from the University of SGBAU, Amravati, India, and his Ph.D. degree in Engineering and Technology from the University of SGBAU, Amravati, India, in 2003 and 2013, respectively. From 1999 to 2018 he was at the University of Amravati and Nagpur, as Assistant Professor. He is currently an Associate Professor in the Department of Electronics Engineering, the University of SGBAU, and Amravati, India.